JOURNAL OF AIRCRAFT
Vol. 37, No. 2, March–April 2000

Strength of 2024-T3 Aluminum Panels with Multiple Site Damage

Bert L. Smith,* Perry A. Saville,† Adil Mouak,† and Roy Y. Myose‡
Wichita State University, Wichita, Kansas 67220-0044

An aging aircraft accumulates fatigue cracks commonly referred to as multiple site damage (MSD). For ductile materials such as 2024-T3 aluminum, MSD cracks may lower the strength significantly below that which is predicted by conventional fracture mechanics or net section yield failure methods. An analytical model generally referred to as the linkup model (or the plastic-zone-touch model) has previously been used to describe the MSD phenomenon. However, the linkup model is only accurate for limited geometric configurations. Two modifications to the linkup model were developed through regression analysis of test data obtained from the literature and from experimental results conducted in this investigation. The modified models show significantly improved correlation with the test data over a wide range of configurations for flat 2024-T3 aluminum panels with MSD at open holes.

Nomenclature

a = lead crack half-length
a_n = nominal lead crack half-length
c = MSD crack length
D = hole diameter
L = ligament length
ℓ = half-length for MSD crack and hole, $c + D/2$
t = panel thickness
W = panel width
β_a = correction to stress intensity of the lead crack, $\beta_{a/\ell}\beta_W$
$\beta_{a/\ell}$ = correction to stress intensity of the lead crack for the effect of the adjacent MSD crack
β_b = correction to stress intensity of the adjacent MSD crack for the effect of an open hole
β_ℓ = correction to stress intensity of the adjacent MSD crack, $\beta_{\ell/a}\beta_b\sqrt{(c/\ell)}$
$\beta_{\ell/a}$ = correction to stress intensity of the adjacent MSD crack for the effect of the lead crack
β_W = finite-width correction to the stress intensity of the lead crack, $\sqrt{[\sec(\pi a/w)]}$
σ_c = critical stress for ligament failure based on modified linkup
σ_{LU} = critical stress for ligament failure based on linkup, $\sigma_{ys}\sqrt{[2L/(a\beta_a^2 + \ell\beta_\ell^2)]}$
σ_{Test} = critical stress for ligament failure obtained from testing
σ_{ys} = yield strength

Introduction

AN aging aircraft accumulates fatigue damage in the form of small-scale cracking at places of high stress concentration. This type of damage is commonly referred to as multiple site damage (MSD). Panels with major (lead) cracks exhibit a loss in strength. However, panels with MSD in addition to major cracks may exhibit a further loss in strength, especially panels of ductile materials such as 2024-T3 aluminum. Until recently the additional loss in strength caused by MSD was often ignored. In an attempt to explain this phenomenon, Swift[1] described an analytical model called the linkup model or the plastic-zone-touch model. The linkup model clearly shows an additional loss in strength from MSD. However, it does not accurately predict the magnitude of the loss for many geometric configurations, as will be shown later in the paper. Thus, there is a need to examine the linkup model further and to improve the model so that it predicts accurate results for a wide range of parameters. The objectives of this investigation are to ascertain the accuracy of the linkup model and to modify it as necessary to fit test data. An empirical approach is taken to satisfy the needs of engineers in the aircraft industry for a simple but accurate method to determine the strength of thin 2024-T3 aluminum panels with MSD.

Three different modifications to the linkup model were developed,[2–5] based on test data from 40 different flat unstiffened panels with MSD. Excellent results were obtained from the first of these modified models.[2,4] However, this model requires the fracture toughness of the panel material, and, furthermore, it is not as easy to use as the later two models. Therefore, it is not discussed in this paper. The later two modified linkup models, referred to herein as Wichita State University (WSU) linkup models 2 and 3 (or simply WSU2 and WSU3), are easier to use and still give accurate results for a large range of parameters including panel thickness and width, lead crack length, MSD crack length, and ligament length. Initially, these modified linkup models were developed using yield strength values of the panels as reported by the sources from which the test data were obtained. In practice, however, engineers would most likely use handbook values for the yield strength. Thus, the modified linkup models were redeveloped using MIL-HDBK-5G yield strength values, and the results of this redevelopment are discussed here. The results of this investigation should add to the understanding of the extent to which nonlinear behavior can be described by simplified engineering models.

Linkup Model

A schematic diagram of a panel with multiple site damage is shown in Fig. 1. It has a central lead crack of length 2a and collinear MSD cracks emerging from the adjacent holes. A value of the remote stress that produces crack extension and ligament failure is referred to herein as a critical stress. There are several possible modes that can produce crack extension and ligament failure, depending upon the panel and crack configuration. For each of these modes, a critical value of the remote stress σ may be determined, and crack extension with ligament failure will occur according to the mode with the smallest stress. One of the modes is based on linear elastic fracture mechanics, and another mode is based on net section yielding. Ductile materials such as 2024-T3 aluminum, in the presence of MSD, often fail at stresses below these two modes. Thus, a third mode called the linkup (or plastic-zone-touch) mode has been identified, and the critical stress for this mode is identified as σ_{LU}. The critical stress for ligament failure for the linkup mode is given in Eq. (1) as follows[1]:

$$\sigma_{LU} = \sigma_{ys}\sqrt{2L/(a\beta_a^2 + \ell\beta_\ell^2)} \tag{1}$$

Received 18 January 1999; revision received 8 July 1999; accepted for publication 27 July 1999.

*Professor, Department of Aerospace Engineering.
†Graduate Research Assistant, Department of Aerospace Engineering; currently Engineer, Cessna Aircraft Co. 178 WIN-9, P.O. Box 7704, Wichita, KS 67277.
‡Associate Professor, Department of Aerospace Engineering. Associate Fellow AIAA.

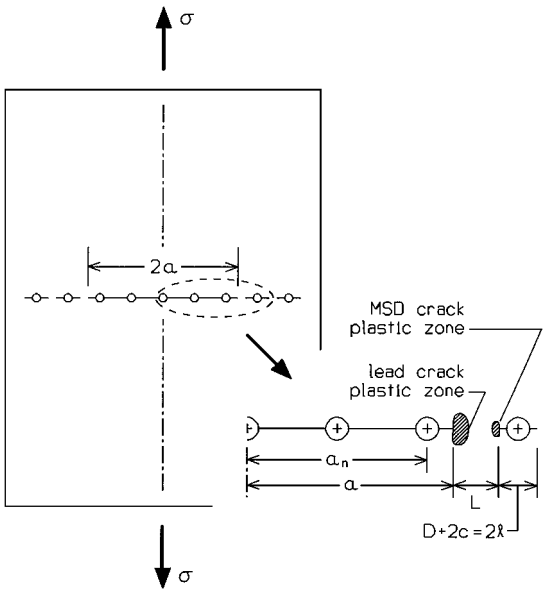

Fig. 1 Panel configuration.

The corrections to stress intensity of the lead crack and adjacent MSD crack are given by

Lead crack:

$$\beta_a = \beta_{a/\ell}\beta_W \tag{2}$$

Adjacent MSD crack:

$$\beta_\ell = \beta_{\ell/a}\beta_b\sqrt{c/\ell} \tag{3}$$

The correction to the stress intensity of the lead crack for the effect of the adjacent MSD crack is $\beta_{a/\ell}$ (Ref. 6), and β_W is the finite-width correction to the stress intensity of the lead crack $\{\beta_W = \sqrt{\sec(\pi a/w)}\}$. The correction to the stress intensity of the adjacent MSD crack for the effect of the lead crack is $\beta_{\ell/a}$ (Ref. 6), and β_b is the correction for open holes (Ref. 7), which is given by

$$\beta_b = 1 - \frac{0.15}{1 + 2c/d} + \frac{3.46}{(1 + 2c/d)^2} - \frac{4.47}{(1 + 2c/d)^3} + \frac{3.52}{(1 + 2c/d)^4} \tag{4}$$

Equation (1) is based on the concept that ligament failure will occur when the remote stress σ reaches a level that causes the surfaces of the lead-crack-tip plastic zone and the adjacent MSD crack-tip plastic zone (Fig. 1) to touch. Unfortunately, the linkup model has proven to be unreliable, as will be shown later. It is accurate for some configurations, but highly inaccurate for others. This project involved the development of a wide spectrum of test data and a subsequent empirical analysis to modify the linkup model to fit the test data.

Experimental Setup

Twenty-nine 24-in. wide 2024-T3 aluminum panels were tested for (ligament failure) critical strengths at WSU. These 29 panels yielded test values for 22 different configurations (combinations of lead crack length and MSD crack length). Eighteen additional critical strength values were obtained from the literature, including nine from the National Institute of Standards and Technology[8] (NIST) and nine more from Foster-Miller[9] (F-M). The NIST panels were 90 in. wide, whereas the F-M panels were 20 in. wide. Thus, test results for a total of 40 different panel and crack configurations were obtained.

A servo-hydraulic testing machine was used to test the aluminum panels at WSU. Figure 2 shows a test panel along with test fixturing. These 24-in. wide panels were 0.063 in. thick and 36 in. long. Midspan fixtures were used to prevent buckling along the crack line,

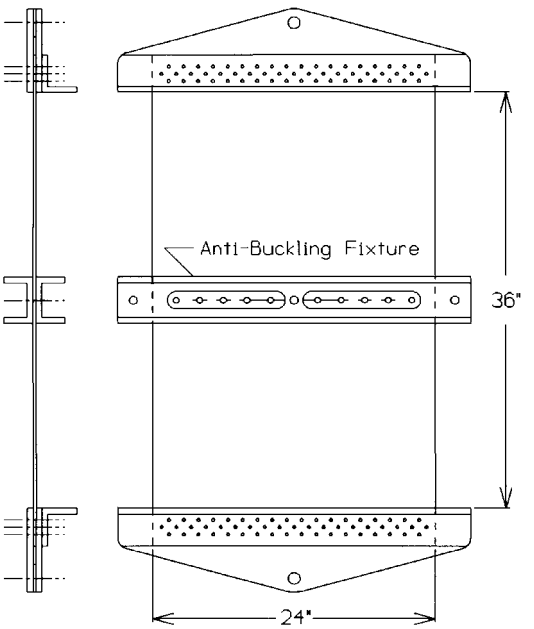

a) Side and front view schematic diagram of test setup

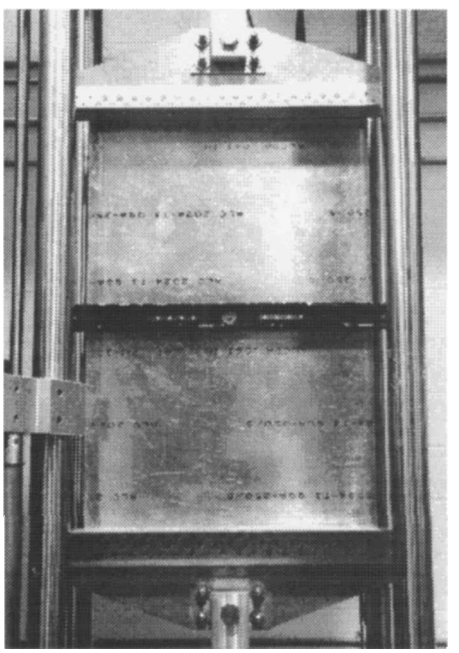

b) Photograph of actual test panel in the servo-hydraulic test machine

Fig. 2 Test setup.

and heavy stiffeners were used at each end to help distribute the load evenly across the width.

During the early stages of testing, both stroke control and load control were used, producing identical results. Thus, stroke control was used thereafter at a rate of 0.01 in. per minute. Real-time observations were made using a closed-circuit television system, which allowed magnified viewing of the lead crack and adjacent MSD crack. The observed test results were recorded by a charge couple device camera and S-VHS video recorder. A time code generator imprinted a time reference on the video every $\frac{1}{30}$ of a second. This allowed frame-by-frame viewing of the recorded images and comparison against quantitative measurements of load vs time made by the servo-hydraulic test machine.

The man-made MSD cracks were produced by Electro Discharge Machine (EDM) with a 0.004-in.-diam wire resulting in actual crack widths of 0.005 in. The saw cuts in the NIST panels were 0.003 in.

in width and those in the F-M panels were 0.006 in. in width. Panels with cracks produced by a jeweler's saw were also tested at WSU; however, the results were not as consistent as the machine-controlled EDM cracks. There has been a concern as to whether crack tips produced by EDM or saw cuts may be used to produce reliable results for residual strength tests, as compared with results produced from fatigue cracked specimens. Dawicke et al.[10] demonstrated a significant difference in the results between using these two types of cracks. On the other hand, Heinimann[11] and Secton[12] concluded that narrow EDM slots less than 0.005 in. wide provided a suitable comparative method for residual strength tests requiring consistent initial configurations. Thus, this issue is unresolved. Based on the observation that EDM (and saw-cut) cracks in 2024-T3 panels undergo stable crack extension and become real cracks prior to ligament failure, the decision was made to use EDM cracks rather than fatigue cracks. Also, precise initial configurations could be achieved much easier with EDM cracks than with fatigue cracks.

Initially, three panels of each crack configuration were tested at WSU. However, the results were so consistent that this procedure was abandoned and the remaining panels were used for different crack configurations. Each panel was cut from an oversized aluminum sheet so that the yield strength could be obtained from the excess material. Tables 1 and 2 give detailed information about each of the 40 different panel configurations. Table 2 also gives A-basis and B-basis yield strength values from MIL-HDBK-5G for each of the panel configurations. Additional details about the panels tested by the NIST and F-M are given in Refs. 8 and 9, respectively.

Table 1 Panel configuration

Panel ID	Source	MSD type	Crack type	W, in.	D, in.	a, in.	c, in.	L, in.
1	NIST	hole	saw cut	90	0.221	10.00	0.14	0.25
2	NIST	hole	saw cut	90	0.221	7.00	0.09	0.30
3	NIST	hole	saw cut	90	0.221	2.80	0.19	0.40
4	NIST	hole	saw cut	90	0.221	7.70	0.09	0.60
5	NIST	hole	saw cut	90	0.221	9.50	0.14	0.75
6	NIST	hole	saw cut	90	0.221	3.80	0.19	0.90
7	NIST	hole	saw cut	90	0.221	10.75	0.14	1.00
8	NIST	hole	saw cut	90	0.221	10.75	0.14	1.00
9	NIST	hole	saw cut	90	0.221	5.00	0.09	1.30
10	WSU	hole	EDM	24	0.25	3.675	0.05	0.15
11	WSU	hole	EDM	24	0.25	3.575	0.05	0.25
12	WSU	hole	EDM	24	0.25	3.475	0.05	0.35
13	WSU	hole	EDM	24	0.25	3.325	0.20	0.35
14	WSU	hole	EDM	24	0.25	3.275	0.15	0.45
15	WSU	hole	EDM	24	0.25	3.225	0.10	0.55
16	WSU	hole	EDM	24	0.25	3.175	0.05	0.65
17	WSU	hole	EDM	24	0.25	4.675	0.05	0.15
18	WSU	hole	EDM	24	0.25	4.575	0.05	0.25
19	WSU	hole	EDM	24	0.25	4.475	0.05	0.35
20	WSU	hole	EDM	24	0.25	4.325	0.20	0.35
21	WSU	hole	EDM	24	0.25	4.275	0.15	0.45
22	WSU	hole	EDM	24	0.25	4.225	0.10	0.55
23	WSU	hole	EDM	24	0.25	4.175	0.05	0.65
24	WSU	hole	EDM	24	0.25	5.675	0.05	0.15
25	WSU	hole	EDM	24	0.25	5.575	0.05	0.25
26	WSU	hole	EDM	24	0.25	5.475	0.05	0.35
27	WSU	hole	EDM	24	0.25	5.325	0.20	0.35
28	WSU	hole	EDM	24	0.25	5.275	0.15	0.45
29	WSU	hole	EDM	24	0.25	5.225	0.10	0.55
30	WSU	hole	EDM	24	0.25	5.175	0.05	0.65
31	WSU	hole	EDM	24	0.25	6.325	0.20	0.35
32	F-M	slit	saw cut	20	——	4.00	——	0.35
33	F-M	slit	saw cut	20	——	3.80	——	0.45
34	F-M	slit	saw cut	20	——	1.60	——	0.50
35	F-M	slit	saw cut	20	——	2.50	——	0.50
36	F-M	slit	saw cut	20	——	3.70	——	0.55
37	F-M	slit	saw cut	20	——	1.60	——	0.65
38	F-M	slit	saw cut	20	——	3.60	——	0.65
39	F-M	slit	saw cut	20	——	3.00	——	1.25
40	F-M	slit	saw cut	20	——	1.50	——	1.50

Table 2 Panel material information

Panel ID	Source	Bare or clad	Load direction[a]	t, in.	A-basis σ_{ys}, ksi	B-basis σ_{ys}, ksi
1	NIST	Bare	L	0.04	47	48
2	NIST	Bare	L	0.04	47	48
3	NIST	Bare	L	0.04	47	48
4	NIST	Bare	L	0.04	47	48
5	NIST	Bare	L	0.04	47	48
6	NIST	Bare	L	0.04	47	48
7	NIST	Bare	L	0.04	47	48
8	NIST	Bare	L	0.04	47	48
9	NIST	Bare	L	0.04	47	48
10	WSU	Clad	L	0.063	45	47
11	WSU	Clad	L	0.063	45	47
12	WSU	Clad	L	0.063	45	47
13	WSU	Clad	LT	0.063	40	42
14	WSU	Clad	LT	0.063	40	42
15	WSU	Clad	LT	0.063	40	42
16	WSU	Clad	LT	0.063	40	42
17	WSU	Clad	LT	0.063	40	42
18	WSU	Clad	LT	0.063	40	42
19	WSU	Clad	LT	0.063	40	42
20	WSU	Clad	LT	0.063	40	42
21	WSU	Clad	LT	0.063	40	42
22	WSU	Clad	LT	0.063	40	42
23	WSU	Clad	LT	0.063	40	42
24	WSU	Clad	L	0.063	45	47
25	WSU	Clad	L	0.063	45	47
26	WSU	Clad	L	0.063	45	47
27	WSU	Clad	LT	0.063	40	42
28	WSU	Clad	LT	0.063	40	42
29	WSU	Clad	LT	0.063	40	42
30	WSU	Clad	LT	0.063	40	42
31	WSU	Clad	LT	0.063	40	42
32	F-M	Clad	LT	0.04	39	40
33	F-M	Clad	LT	0.04	39	40
34	F-M	Clad	LT	0.04	39	40
35	F-M	Clad	LT	0.04	39	40
36	F-M	Clad	LT	0.04	39	40
37	F-M	Clad	LT	0.04	39	40
38	F-M	Clad	LT	0.04	39	40
39	F-M	Clad	LT	0.04	39	40
40	F-M	Clad	LT	0.04	39	40

[a]L = longitudinal grain direction and LT = long transverse grain direction as per MIL-HDBK-5G.

Empirical Analysis of Test Data

The calculated linkup stresses from Eq. (1) using A-basis yield strength values and the test results are given in Table 3. Where duplicates were tested, the test value in Table 3 represents the average value. The average error (i.e., the absolute value of the difference) between σ_{Test} and σ_{LU} is 14.2%. An empirical approach was taken to try to modify and improve the linkup model so that it would fit the test data and improve the accuracy. Three different improved models (or modifications) were developed. However, the first of these three has since been abandoned as already discussed, and only the latter two, referred to herein as WSU linkup models 2 and 3 (or simply WSU2 and WSU3), will be described.

After investigating a large number of test cases, it became apparent that the ligament length strongly influences the linkup stress σ_{LU}. Therefore, the data were displayed as illustrated in Fig. 3 with the ligament size plotted on the horizontal axis and the difference between linkup stress and test value divided by test value plotted on the vertical axis. Although there is some scatter in the data, a reasonably good representation of the data can be made with a single equation of the natural log form. When the data are represented by a single curve, the stress σ_{Test} becomes the critical stress for WSU2 as follows:

$$(\sigma_{LU} - \sigma_C)/\sigma_C = C_1[\ell n(L)] + C_2 \tag{5}$$

or WSU2:

$$\sigma_C = \sigma_{LU}/\{C_1[\ell n(L)] + (C_2 + 1)\} \tag{6}$$

Table 3 Critical stresses (based on A-basis yield strengths)

Panel ID	σ_{LU}, ksi	Broek σ_c, ksi	LMC σ_c, ksi	WSU2 σ_c, ksi	WSU3 σ_c, ksi	σ_{Test}, ksi
1	8.49	——	10.37	9.56	10.44	8.92
2	11.50	——	12.73	12.19	12.64	12.20
3	20.37	——	16.69	19.75	18.06	20.00
4	16.53	——	15.77	14.30	16.24	14.20
5	16.55	——	15.73	13.52	16.22	12.90
6	28.63	——	21.13	22.36	23.48	23.40
7	18.23	——	16.61	13.89	17.36	13.20
8	18.23	——	16.61	13.89	17.36	13.30
9	31.75	——	23.05	22.80	25.69	22.00
10	9.19	——	10.28	12.57	10.19	11.58
11	13.18	——	12.93	14.88	13.20	14.09
12	16.54	——	14.76	16.69	15.53	16.27
13	13.89	12.11	12.26	14.03	12.95	13.67
14	16.86	14.43	13.94	15.79	15.04	15.96
15	19.56	16.45	15.41	17.32	16.86	17.41
16	22.39	18.51	16.99	18.97	18.77	19.22
17	7.17	6.52	8.41	9.80	8.35	9.80
18	10.14	9.10	10.60	11.43	10.63	12.09
19	12.64	11.18	12.04	12.76	12.41	13.77
20	11.92	10.53	11.26	12.04	11.63	11.94
21	14.45	12.59	12.75	13.53	13.47	14.09
22	16.75	14.40	14.03	14.84	15.08	15.33
23	19.05	16.15	15.31	16.14	16.66	17.37
24	7.02	——	8.51	9.60	8.53	8.56
25	9.93	——	10.88	11.19	10.81	10.73
26	12.39	——	12.44	12.51	12.61	12.14
27	10.40	9.27	10.37	10.50	10.53	10.33
28	12.58	11.08	11.71	11.78	12.16	12.11
29	14.47	12.61	12.77	12.82	13.49	13.62
30	16.47	14.19	13.92	13.96	14.91	15.77
31	9.14	8.19	9.52	9.22	9.55	10.33
32	13.26	11.97	12.27	13.39	12.76	14.13
33	15.01	13.31	12.86	14.06	13.72	14.50
34	23.64	19.05	16.66	21.49	18.62	21.00
35	18.25	15.51	13.91	16.59	15.35	15.38
36	17.23	15.04	13.99	15.26	15.18	16.00
37	29.71	23.03	20.19	25.18	22.57	24.88
38	19.26	16.53	14.99	16.31	16.46	17.25
39	31.02	23.94	21.01	22.47	23.48	22.50
40	44.66	28.85	27.96	31.09	30.19	28.25

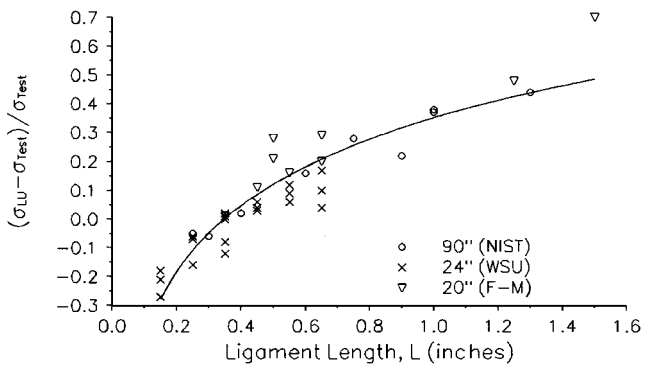

Fig. 3 Natural log form correction used for WSU2.

In Eq. (6) the stresses σ_c and σ_{LU} are in units of ksi, and the ligament length is in inches. The coefficients C_1 and C_2 in Eq. (6) were determined from an empirical analysis based on MIL-HDBK-5G yield strength values as given in Table 2. For A-basis yield strength values the coefficients in Eq. (6) are $C_1 = 0.3065$ and $C_2 = 0.3123$ as shown in Fig. 3. The figure for the B-basis log form fit, although not shown, is similar in appearance. For B-basis yield strength values the coefficients are $C_1 = 0.3054$ and $C_2 = 0.3502$.

A nondimensionalized version of Eq. (6) was developed through a similar empirical analysis. This analysis is shown graphically in Fig. 4, where the horizontal axis is a/L rather than L. The curve fit shown in Fig. 4 leads to the following equations:

$$(\sigma_{LU} - \sigma_C)/\sigma_C = C_3[\ln(a/L)] + C_4 \tag{7}$$

WSU3:

$$\sigma_C = \sigma_{LU}/[C_3 \ln(a/L) + (C_4 + 1)] \tag{8}$$

For A-basis yield strength values the coefficients in Eq. (8) are $C_3 = -0.1806$ and $C_4 = 0.4791$ as shown in Fig. 4. The figure for the B-basis log form fit, although not shown, is similar in appearance. For B-basis yield strength values the coefficients are $C_3 = -0.1813$ and $C_4 = 0.5193$.

Table 4 Critical stresses (based on B-basis yield strengths)

Panel ID	σ_{LU}, ksi	Broek σ_c, ksi	LMC σ_c, ksi	WSU2 σ_c, ksi	WSU3 σ_c, ksi
1	8.67	——	10.59	9.35	10.19
2	11.75	——	13.00	11.96	12.39
3	20.80	——	17.05	19.43	17.83
4	16.88	——	16.10	14.14	15.98
5	16.90	——	16.07	13.39	15.96
6	29.24	——	21.58	22.18	23.24
7	18.62	——	16.96	13.79	17.10
8	18.62	——	16.96	13.79	17.10
9	32.42	——	23.54	22.67	25.43
10	9.59	——	10.74	12.45	10.21
11	13.77	——	13.51	14.86	13.28
12	17.27	——	15.41	16.77	15.66
13	14.59	12.11	12.88	14.17	13.13
14	17.70	14.43	14.64	16.00	15.27
15	20.53	16.45	16.18	17.59	17.13
16	23.51	18.51	17.84	19.29	19.09
17	7.52	6.52	8.84	9.76	8.40
18	10.65	9.10	11.13	11.49	10.73
19	13.27	11.18	12.65	12.89	12.55
20	12.52	10.53	11.82	12.16	11.77
21	15.17	12.59	13.39	13.71	13.65
22	17.59	14.40	14.74	15.07	15.30
23	20.00	16.15	16.08	16.41	16.92
24	7.33	——	8.89	9.51	8.52
25	10.37	——	11.36	11.19	10.85
26	12.94	——	13.00	12.57	12.68
27	10.92	9.27	10.89	10.61	10.64
28	13.20	11.08	12.30	11.93	12.31
29	15.20	12.61	13.41	13.01	13.68
30	17.30	14.19	14.61	14.19	15.13
31	9.59	8.19	9.99	9.32	9.65
32	13.60	11.97	12.59	13.21	12.62
33	15.39	13.31	13.19	13.91	13.59
34	24.24	19.05	17.09	21.29	18.53
35	18.71	15.51	14.26	16.44	15.25
36	17.67	15.04	14.35	15.13	15.06
37	30.48	23.03	20.71	25.01	22.47
38	19.75	16.53	15.37	16.21	16.34
39	31.82	23.94	21.55	22.43	23.38
40	45.81	28.85	28.68	31.07	30.15

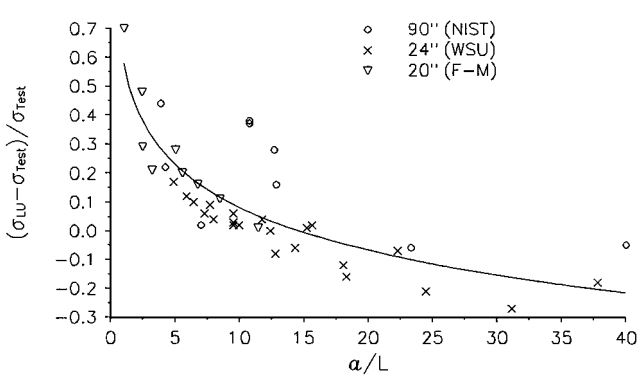

Fig. 4 Nondimensional natural log form correction used for WSU3.

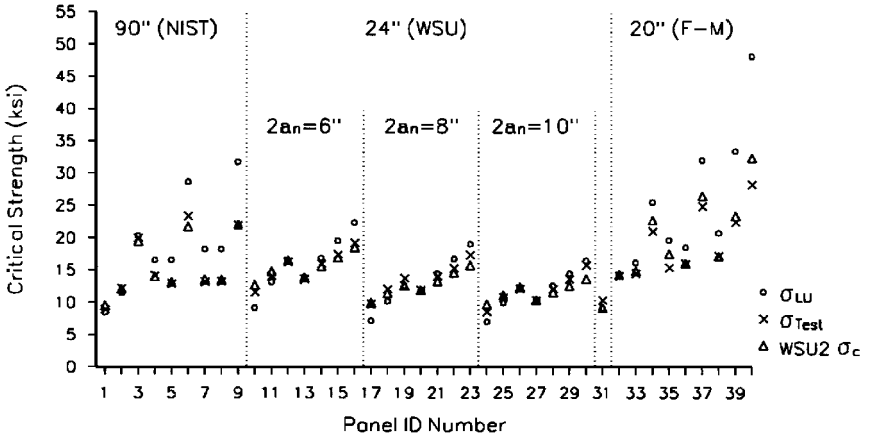

Fig. 5 Panel stresses compared to WSU2 for A-basis empirical analysis.

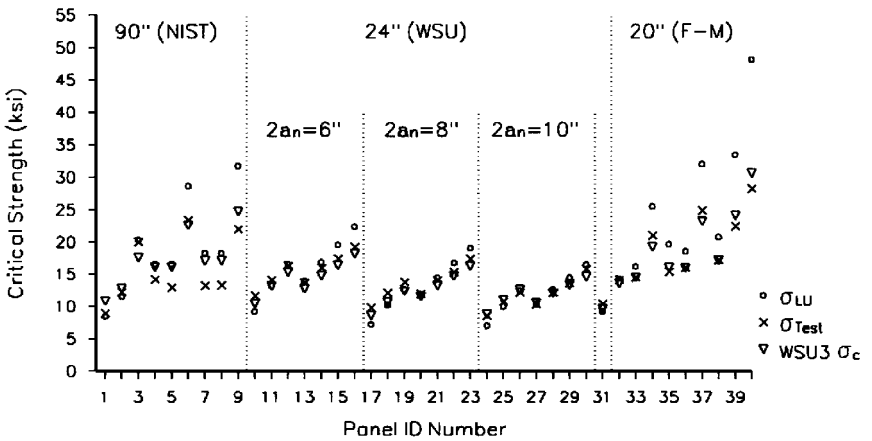

Fig. 6 Panel stresses compared to WSU3 for A-basis empirical analysis.

Two other modified linkup models have been developed and reported in the literature, one by Broek[13] and the other more recently by Ingram et al.[14] of Lockheed Martin Corporation (LMC). These models are given as follows:

Broek:

$$\sigma_C = \{0.5 + 0.9[1/(1 + L/a)]\}F_{\text{col}}\sqrt{L/(a\beta_a^2 + \ell\beta_\ell^2)} \quad (9)$$

LMC:

$$\sigma_C = (1.83 - e^{-0.057a/L})\sigma_{\text{ys}}\sqrt{L/(a\beta_a^2 + \ell\beta_\ell^2)} \quad (10)$$

The Broek model of Eq. (9) was developed from an empirical analysis based on the test data from the F-M panels. The collapse stress F_{col} was determined by Broek as 37.5 ksi for the 2024-T3 material. The test database for this model included only clad material, a single panel thickness of 0.04 in., and loading in the long transverse (LT) grain direction. The LMC model of Eq. (10) was devloped from an empirical analysis based on test data from the F-M panels, the NIST panels, and the WSU panels. This model was also based on yield strength values reported by F-M, NIST, and WSU, rather than MIL-HDBK-5G values.

Results

The A-basis yield strength results for the modified linkup models (Broek, LMC, WSU2, and WSU3) are given in Table 3, whereas the B-basis yield strength results are given in Table 4. The Broek model of Eq. (9) is not dependent upon the MIL-HDBK-5G yield strengths, but rather a collapse stress of 37.5 ksi. However, results from the Broek model have been put in Tables 3 and 4 for comparison purposes. Results for the Broek model are only given for clad material with loading in the LT direction as already discussed. Results for the LMC model are included in these tables even though this model was developed based on yield strength values reported by F-M, NIST, and WSU, rather than MIL-HDBK-5G values as already discussed.

Figure 5 is a plot of panel identification (ID) number vs the critical stress obtained from testing and the A-basis yield strength results for the linkup model and the WSU2 model. Figure 6 is the same except that the WSU3 stresses are shown rather than the WSU2 stresses. In each figure the first nine IDs are the 90-in. panels tested by the NIST, the next 22 IDs are the 24-in. panels from WSU, and the final nine IDs are the 20-in. panels from F-M. The NIST and the F-M panels are arranged in order of increasing ligament length. The panels tested at WSU are arranged in groups of nominal lead crack length $2a_n$, and within each of these groups they are arranged in order of increasing ligament length. The symbol x represents the test values, the circles represent analytical results predicted by the linkup model, while the triangles represent analytical results determined from the WSU2 model in Fig. 5 and the WSU3 model in Fig. 6. The two modified linkup models (WSU2 and WSU3) give significantly better results than the original linkup model over this wide spectrum of configurations.

For each panel configuration the absolute value of the difference between the test result and each of the different analytical models was determined. These absolute values are positive quantities and are referred to as errors. The average error based on the 40 different panel configurations for each of the five different analytical models (LU, Broek, LMC, WSU2, and WSU3) is given in Table 5. The analytical values vs the test values are shown for each of the analytical models in Figs. 7–11 for the A-basis yield strength analysis. For the Broek model an exception was made; only the 24 panels in Table 2

Table 5 Average error between test result and different analytical models

Analytical model	Average error based on A-basis σ_{ys},%	Average error based on B-basis σ_{ys},%
LU, Eq. (1)	14.16	16.09
Broek, Eq. (9)	10.38[a]	10.38[a]
LMC, Eq. (10)	10.63	9.06
WSU2, Eq. (6)	4.34	4.09
WSU3, Eq. (8)	7.90	7.34

[a]The collapse stress of 37.5 ksi is used rather than the yield strength in the case of Broek's model.

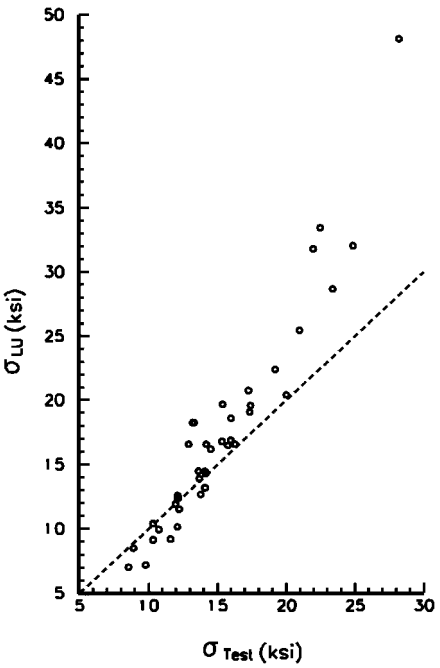

Fig. 7 Test results compared to linkup stresses.

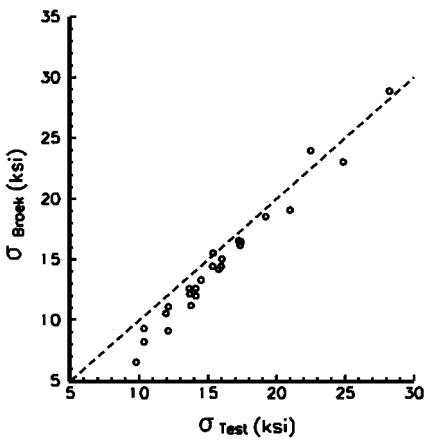

Fig. 8 Test results compared to Broek model.

with the clad surface and the load in the LT grain direction were used. The corresponding figures for the B-basis yield strength analysis, although not shown, are similar in appearance. In each case the ideal situation would be for all of the points to fall on a 45-deg line. This is the case more so for the LMC and the two WSU models than for the other two. Figure 8 shows that the Broek model is consistently conservative, whereas Fig. 7 shows the unmodified linkup model to be conservative for lower stresses and unconservative for higher stresses. The LMC and the two WSU models cluster along the 45-deg line better.

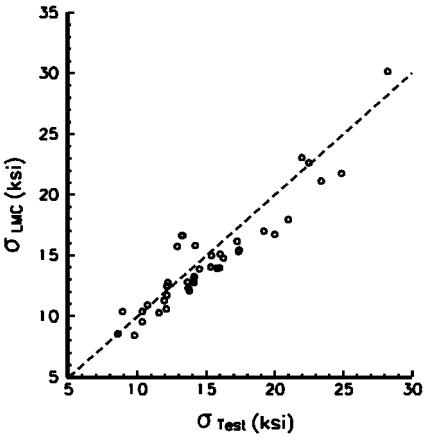

Fig. 9 Test results compared to LMC model.

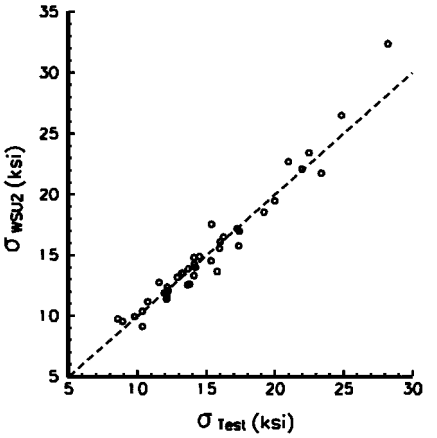

Fig. 10 Test results compared to WSU2 model.

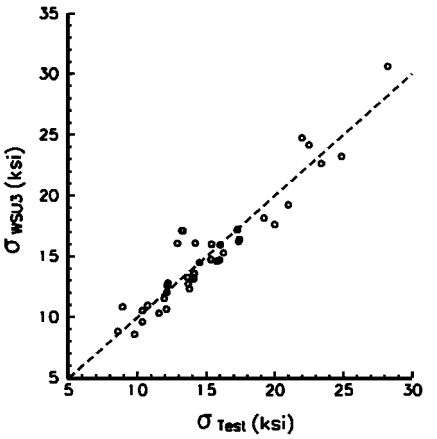

Fig. 11 Test results compared to WSU3 model.

Conclusions

In this study three different panel widths, two different panel thicknesses, lead crack half-lengths ranging from 1.5 to 10.75 in., MSD crack lengths ranging from 0.05 to 0.20 in., ligament lengths ranging from 0.15 to 1.5 in., two different grain directions, two different surface conditions (clad and bare), and material originating from different lots were considered. This is indeed a very wide range of parameters. However, only one alloy, 2024-T3 aluminum, was used in this study. Thus, there is no assurance that the modified linkup models developed in this study will apply to other alloys.

The original linkup model is accurate for predicting the critical (linkup) stress for certain crack configurations, but highly inaccurate

for others. It appears to give conservative results for configurations with short ligaments and unconservative results for configurations with long ligaments. However, the improved models of Eqs. (6), (8), and (10) give more accurate results for a large envelope of configurations covering a variety of panel widths and thicknesses, lead crack lengths, MSD crack lengths, and ligament lengths for flat 2024-T3 aluminum panels with MSD at open holes.

Recently, this project has been extended to evaluate the accuracy of the improved models for panels with stiffeners. Preliminary results[4,5] indicate that both WSU2 and WSU3 as well as the LMC model predict the critical strength of stiffened panels with MSD much more accurately than the original linkup model.

Acknowledgments

This work was sponsored by the industrial members of the Aircraft Design and Manufacturing Research Center of Wichita State University, Wichita, Kansas. The material for the aluminum panels was donated by Alcoa Aerospace Center, Hutchinson, Kansas, and EDM cracks were produced by the Materials Testing Laboratory of the Boeing Company, Wichita, Kansas. Their support is greatly appreciated. Thanks go to Ala Hijazi and A. K. M. Haque for their help in revising the analytical models for use with A- and B-basis yield strength values.

References

[1]Swift, T., "Widespread Fatigue Damage Monitoring Issues and Concerns," 5th International Conf. on Structural Airworthiness of New and Aging Aircraft, June 1993.

[2]Smith, B., Camenzind, J., Myose, R., Saville, P., Mouak, A., and Horn, W., "The Effect of Multiple Site Damage on the Critical Strength of Aluminum Panels," *Developments in Theoretical and Applied Mechanics*, Vol. 19, 1998, pp. 421–429; also *Proceedings of the Nineteenth Southeastern Conference on Theoretical and Applied Mechanics*, 1998.

[3]Smith, B. L., Saville, P. A., Mouak, A., Myose, R. Y., and Horn, W. J., "A Further Study on the Effect of Multiple Site Damage on the Critical Strength of Aluminum Panels," *Proceedings of the Twelfth ASCE Engineering Mechanics Conference*, 1998, pp. 626–629.

[4]Smith, B., Mouak, A., Saville, P., Myose, R., and Horn, W., "Improved Engineering Methods for Determining the Critical Strength of Aluminum Panels with Multiple Site Damage," *Proceedings of the Second Joint NASA/FAA/DoD Conference on Aging Aircraft*, edited by Charles E. Harris, Langley Research Center, Hampton, VA, Jan. 1999, pp. 525–534; also NASA CP-1999-208982.

[5]Smith, B., Mouak, A., Saville, P., Hijazi, A., and Myose, R., "Strength of Stiffened Panels with Multiple Site Damage," Society of Automatic Engineers Paper 1999-01-1575, April 1999.

[6]Rooke, D. P., and Cartwright, D. J., *Compendium of Stress Intensity Factors*, Her Majesty's Stationary Office, London, 1976.

[7]Newman, J. C., Jr., "Predicting Failure of Specimens with Either Surface Cracks or Corner Cracks at Holes," NASA TN D-8244, June 1976.

[8]Fields, R., Low, S., III, Harne, D., and Froecke, T., "Fracture Testing of Large-Scale Thin-Sheet Aluminum Alloy," National Inst. of Standards and Technology, NISTIR 5661, Gaithersburg, MD, May 1995.

[9]Thompson, D., Hoadley, D., and McHatton, J., "Load Tests of Flat and Curved Panels with Multiple Cracks," Foster-Miller, Inc. (prepared for FAA), Waltham, MA, Sept. 1993.

[10]Dawicke, D. A., Newman, J. C., Jr., Sutton, M. A., and Amstutz, B. E., "Stable Tearing Behavior of a Thin Sheet Material with Multiple Cracks," NASA TM-109131, July 1994.

[11]Heinimann, M. B., "Analysis of Stiffened Panels with Multiple Site Damage," Ph.D. Dissertation, School of Aeronautics and Astronautics, Purdue Univ., West Lafayette, IN, May 1997.

[12]Secton, D. G., "A Comparison of Fatigue Damage Resistance and Residual Strength of 2024-T3 and 2524-T3 Panels Containing Multiple Site Damage," M.S. Thesis, School of Aeronautics and Astronautics, Purdue Univ., West Lafayette, IN, May 1997.

[13]Broek, D., "The Effects of Multi-Site Damage on the Arrest Capability of Aircraft Fuselage Structure," FractuResearch, TR 9302, Galena, OH, June 1993.

[14]Ingram, J. E., Kwon, Y. S., Duffié, K. J., and Irby, W. D., "Residual Strength Analysis of Skin Splices with Multiple Site Damage," *Proceedings of the Second Joint NASA/FAA/DoD Conference on Aging Aircraft*, edited by Charles E. Harris, Langley Research Center, Hampton, VA, Jan. 1999, pp. 427–436; also NASA CP-1999-208982.